

Yannis François
Anne Varenne
Juliette Sirieix-Plenet
Pierre Gareil

Laboratory of Electrochemistry
and Analytical Chemistry, UMR
7575 CNRS-ENSCP-Paris6, ENSCP,
Paris, France

Original Paper

Determination of aqueous inclusion complexation constants and stoichiometry of alkyl(methyl)-methylimidazolium-based ionic liquid cations and neutral cyclodextrins by affinity capillary electrophoresis

Affinity CE (ACE) method was developed to characterize the complex formation between seven alkyl(methyl)methylimidazolium-based ionic liquid (IL) cations and eight neutral cyclodextrins (CD). The effective mobility data of the IL cations were processed according to classical nonlinear and linear treatments to obtain the complex stoichiometry and formation constant K . The majority of systems followed a 1:1 complexation stoichiometry model but in four cases a 1:2 stoichiometry was better satisfied. The K values obtained for each IL were compared to elucidate the main influences of IL and CD nature. The availability of these data should lend support to various application areas, including the screening and tailoring of new interactions in the solution for CE.

Keywords: Affinity capillary electrophoresis / Imidazolium based ionic liquids / Inclusion constant / Neutral cyclodextrins / Stoichiometry

Received: September 29, 2006; revised: October 30, 2006; accepted: November 3, 2006

DOI 10.1002/jssc.200600386

1 Introduction

A great interest is being drawn toward ionic liquids (IL) as alternatives for conventional molecular solvents used in organic synthesis and catalytic reactions [1]. They supplement the family of “green solvents” including water and supercritical fluids. Among these, room temperature ionic liquids are defined as materials containing only ionic species and having a melting point lower than 298 K. They exhibit many interesting properties such as negligible vapor pressure, low melting point, large liquid range, unique solvation ability, and overall, the versatility of their physico-chemical properties makes them really attractive. Most of the ILs studied are based on N,N' -dialkylimidazolium cations. They have been recently proposed as solvents in chemical reactions [2–4], multiphase bioprocess operations [5] and liquid–liquid separations [6–8], electrolytes for batteries and fuel cells [9], stationary phases in GC [10–13], mobile

phase additives in LC [14–16], and electrolyte additives in CE [17–26].

Due to their ability to form host–guest inclusion complexes with small molecules, natural and derivatized CDs have been widely used as solubilizing, masking, protecting agents of guest molecules of interest in several application areas including pharmaceutical, health care, fragrance, and as a reagent in a number of analytical methods. The interest of solubilizing CDs as an additive in ILs has also been recognized earlier and few data are already available [11, 27, 28]. To lend support to the development of IL-based processes and to better evaluate the actual benefit that can be obtained from adding CDs, the knowledge of CD–IL interactions is of prime importance. Such data, however, remain scarce. For instance, in the context of the separation of anthraquinones by CE using dialkylimidazolium-based IL and β -CD as additives to BGE, Qi *et al.* [24] suggested the presence of an interaction between analyte and IL cation and between analyte and β -CD, without contemplating the possibility of an interaction between IL cation and β -CD.

Among the different methods available for studying inclusion interactions, mobility shift affinity CE (ACE), based on the alteration of analyte effective mobility due to *in situ* complexation in ligand-containing electrolytes, offers powerful attributes, making it very attractive and well adapted to this task [29–31]. It allows online detec-

Correspondence: Professor Pierre Gareil, Laboratory of Electrochemistry and Analytical Chemistry, UMR 7575 CNRS-ENSCP-UPMC, ENSCP, 11 rue Pierre et Marie Curie, 75231 Paris cedex 05, France

E-mail: pierre-gareil@enscp.fr

Fax: +33-1-44-27-67-50

Abbreviations: ACE, affinity CE; IL, ionic liquid

tion and keeps the consumption of analytes and CDs to a minimum. Other advantages are the short analysis times, the absence of solid phase, high versatility, and the possibility to customize experimental conditions to meet specific needs. Linear, such as Scatchard plot [32, 33] or nonlinear [34] regression analysis of the mobility data as a function of ligand concentration allow to derive the inclusion constant and check stoichiometry.

This work promotes ACE for the quantitative characterization of complexes between a series of imidazolium-based IL cations and neutral CDs in water. This approach should be of interest for various applications, especially in the fields of LC and CE. To generate a broad range of data, seven ILs, differing in the length of the alkyl chain (C_4 – C_{12}) at the N1 position of the imidazolium ring, the presence (or not) of a methyl group at the C2 position of the imidazolium ring and the nature of the IL anion and eight neutral CDs, differing in size and shape of the cavity and external groups close to its rim, were selected.

2 Theoretical

ACE in its mobility shift format has been widely used to study analyte–ligand interactions. This method is a variant of zonal electrophoresis consisting in the injection of a small amount of the analyte of interest while the ligand is present in the running buffer. Provided that the analyte and the ligand have fast association–dissociation kinetics and that the absolute mobilities of the free and bound forms of the analyte are different, then a shift in the position of the analyte peak is expected as the ligand concentration in the running buffer varies.

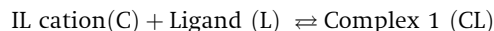
The general ACE approach quantitatively exploits the changes in electrophoretic mobilities of an analyte due to complex formation upon addition of increasing amounts of a ligand to a separation electrolyte. Detailed theoretical treatments and discussions on experimental methods and considerations on the estimation of binding constants can be found in literature [35–37]. Basically, these methods were adapted from similar chromatographic procedures. A molecular association between an analyte and a ligand can be described by the general rectangular hyperbolic form of a binding isotherm

$$y = \frac{ax}{b + cx} \quad (1)$$

The dependent variable y is the experimentally measured response of the analyte–ligand system (in the present case, the effective electrophoretic mobility) while the free variable x is the concentration of free ligand. a , b , and c are constants related to the properties of the analyte, ligand, and complex, respectively, including the complexation constant and stoichiometry information.

2.1 Case of 1:1 complexation equilibrium

A 1:1 complexation equilibrium model was selected *ab initio* to describe the IL cation–CD complex. The complexation equilibrium can then be simply schematized as



The apparent formation constant relative to this equilibrium is

$$K_1 = \frac{[\text{CL}]}{[\text{C}][\text{L}]} \quad (2)$$

where $[\text{CL}]$, $[\text{C}]$, and $[\text{L}]$ are the concentrations of complex 1, free IL cation, and free ligand, respectively.

When a free IL cation is injected in a separation electrolyte containing the ligand, the resulting effective mobility ($\mu_{\text{C}}^{\text{eff}}$) of the IL cation in equilibrium with the ligand is the average of the actual mobilities of the free (μ_{C}^0) and complexed (μ_{CL}^0) forms of the IL cation, weighted by the molar fractions

$$\mu_{\text{C}}^{\text{eff}} = \frac{[\text{C}]}{[\text{CL}] + [\text{C}]} \mu_{\text{C}}^0 + \frac{[\text{CL}]}{[\text{CL}] + [\text{C}]} \mu_{\text{CL}}^0 \quad (3)$$

which, by introducing Eq. (2), can be rearranged to yield the binding isotherm equation

$$\nu \mu_{\text{C}}^{\text{eff}} = \frac{\mu_{\text{C}}^0 + \mu_{\text{CL}}^0 K_1 [\text{L}]}{1 + K_1 [\text{L}]} \quad (4)$$

This equation includes the so-called viscosity correction factor ν [38]

$$\nu = \frac{\eta}{\eta_0} \quad (5)$$

where η is the viscosity of the running buffer containing a given concentration of ligand L and η_0 is the viscosity of the buffer devoid of ligand. Equation (4) allows for accurate calculations of normalized effective mobilities in cases where the viscosity of the running buffer becomes dependent on ligand concentration [37].

Provided that the concentration of the ligand added to the running buffer can be assimilated to the free ligand concentration, Eq. (4) can either be directly handled to obtain complex formation constant by nonlinear least-squares fitting [39] or transformed into four linearized forms, classically referred to as the linearized form of the isotherm and its x -reciprocal, y -reciprocal, and the double reciprocal forms (Table 1) [37]. Although the four linearized equations are equivalent in their algebraic forms, the experimental precision on the free and dependent variables will affect the correlation differently, according to whether they are included in the numerator or the denominator of the equation. For example, the impact of the precision on variable $[\text{L}]$ will alter when the data are transformed to $1/[\text{L}]$ for plotting in the x -reciprocal and double reciprocal methods. Thus these plots give more

Table 1. Linearized forms of the binding isotherm recommended for the determination of binding constants using ACE methods in the mobility shift format [33], case of a 1:1 complexation equilibrium

Method name	Plotting method	K determination	$\mu_{\text{CL}}^0 - \mu_{\text{C}}^0$
Isotherm	$\frac{\mu_{\text{C}}^0 - \mu_{\text{C}}^{\text{eff}}}{\mu_{\text{C}}^{\text{eff}} - \mu_{\text{CL}}^0} = K[\text{L}] = f([\text{L}])$	slope	To be determined by experiment directly
X-reciprocal	$\frac{\mu_{\text{C}}^{\text{eff}} - \mu_{\text{C}}^0}{[\text{L}]} = -K(\mu_{\text{C}}^{\text{eff}} - \mu_{\text{C}}^0) + K(\mu_{\text{CL}}^0 - \mu_{\text{C}}^0) = f(\mu_{\text{C}}^{\text{eff}} - \mu_{\text{C}}^0)$	- Slope	Intercept/slope
Y-reciprocal	$\frac{[\text{L}]}{\mu_{\text{C}}^{\text{eff}} - \mu_{\text{C}}^0} = \frac{1}{\mu_{\text{CL}}^0 - \mu_{\text{C}}^0} \times [\text{L}] + \frac{1}{K(\mu_{\text{CL}}^0 - \mu_{\text{C}}^0)} = f([\text{L}])$	slope/intercept	1/slope
Double reciprocal	$\frac{1}{\mu_{\text{C}}^{\text{eff}} - \mu_{\text{C}}^0} = \frac{1}{K(\mu_{\text{CL}}^0 - \mu_{\text{C}}^0)} \times \frac{1}{[\text{L}]} + \frac{1}{\mu_{\text{CL}}^0 - \mu_{\text{C}}^0} = f\left(\frac{1}{[\text{L}]}\right)$	Intercept/slope	1/intercept

statistical weight to the data collected at the lowest concentrations, where the experimental uncertainty is greater [36]. In addition to the complexation constant, it should be noted that the x -reciprocal, y -reciprocal, and the double reciprocal methods provide the actual mobility of the complexed IL cation μ_{CL}^0 (as far as μ_{C}^0 is easily measured directly), whereas the linearized isotherm method requires the μ_{CL}^0 value to be directly determined experimentally beforehand. A good estimation of the μ_{CL}^0 value can be obtained by measuring the limiting effective mobility of the IL cation at high CD concentration.

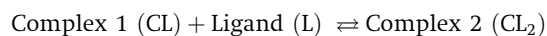
Finally, the experimental verification of the linearity of these plots will ascertain the concordance with a 1:1 complexation equilibrium. It is worth remembering that, more generally, when the assumption of a 1:1 complexation is not made, a Scatchard plot, which is equivalent to an x -reciprocal plot, can give an indication of the stoichiometry of the complexation.

2.2 Case of 1:2 complexation equilibrium

The case of an analyte taking part in 1:1 and 1:2 step by step complexation equilibria in ACE was envisioned by Bowser *et al.* [34]. The effective mobility of an IL cation C involved in such equilibria can then be written

$$\nu\mu_{\text{C}}^{\text{eff}} = \frac{\mu_{\text{C}}^0 + \mu_{\text{CL}}^0 K_1 [\text{L}] + \mu_{\text{CL}_2}^0 K_1 K_2 [\text{L}]^2}{1 + K_1 [\text{L}] + K_1 K_2 [\text{L}]^2} \quad (6)$$

where μ_{C}^0 , μ_{CL}^0 , and $\mu_{\text{CL}_2}^0$ are the actual electrophoretic mobilities of the free, 1:1 complexed, and 1:2 complexed forms of the IL cation, respectively, and K_2 , the step by step formation constant of the 1:2 complex, corresponding to the equilibrium



It can be noted that when only 1:1 complexation takes place, Eq. (6) reduces to Eq. (4).

In order to determine the stoichiometry of IL-CD complexes, these two equations were applied to each system to confirm or cancel the 1:1 equilibrium model, described previously.

3 Experimental

3.1 Chemicals and reagents

1-Ethyl-3-methylimidazolium bis(trifluoromethanesulfonyl)imide (EMIM NTf₂) ($\geq 99\%$) and 1-butyl-3-methylimidazolium bis(trifluoromethanesulfonyl)imide (BMIM NTf₂) ($\geq 99\%$) were a gift from Institut Français du Pétrole (Solaize, France). 1-Butyl-3-methylimidazolium tetrafluoroborate (BMIM BF₄) ($\geq 99\%$), 1-butyl-2,3-dimethylimidazolium tetrafluoroborate (BMMIM BF₄) ($\geq 99\%$), 1-octyl-3-methylimidazolium bromide (C₈MIM Br) ($\geq 99\%$), 1-decyl-3-methylimidazolium tetrafluoroborate (C₁₀MIM BF₄) ($\geq 99\%$) and 1-dodecyl-3-methylimidazolium tetrafluoroborate (C₁₂MIM BF₄) ($\geq 99\%$) were synthesized in our group according to procedures previously reported [40].

α -CD, β -CD, γ -CD, hydroxypropyl- α -CD (HP- α -CD), hydroxypropyl- β -CD (HP- β -CD), and hydroxypropyl- γ -CD (HP- γ -CD), all of three with a degree of substitution (DS) of 0.6 were a kind gift from Wacker-Chemie (Munich, Germany). Heptakis-(2,6-di-*O*-methyl)- β -CD (DM- β -CD) ($>90\%$) and heptakis-(2,3,6-tri-*O*-methyl)- β -CD (TM- β -CD) ($>90\%$) were purchased from Sigma-Aldrich (St. Louis, MO, USA). Sodium acetate was from Prolabo (Fontenay-sous-Bois, France). Glacial acetic acid ($>99\%$), formamide ($>99\%$), and hexadimethrine bromide (Polybrene) were supplied by Aldrich (St. Louis).

3.2 CE instrumentation and methods

All the experiments were performed with an HP^{3D}CE (Agilent Technologies, Waldbronn, Germany) CE system. This apparatus automatically realized all the steps of the measurement protocols, including capillary conditioning, sample introduction, voltage application, and diode array detection, and allowed to run unattended method sequences. A CE Chemstation (Agilent Technologies) was used for instrument control, data acquisition, and data handling. Polymicro bare fused-silica capillaries of 50 µm id were obtained from Photonlines (Marly-le-Roi, France). They were used in 35 cm total length (26.5 cm to detection). Concerning modified capillaries, dynamically coated procedure with polybrene was realized as described in the literature [41–43]. The BGEs were made up with acetic acid/sodium acetate at 30 mM ionic strength in water to a pH of 5.0, containing each CD at various concentrations (zero to 50 mM, depending on the CD). Formamide (0.001% v/v in the BGE) was used as a neutral marker to determine the electroosmotic mobility. The sample solutions were prepared by dissolving each IL at a concentration of *ca.* 2 mM in the aqueous sodium acetate buffer, pH 5.0. New capillaries were conditioned by successive flushes with 1 M and 0.1 M NaOH and then with water under a pressure of 935 mbar, for 10 min each. Before any sample injection, the capillary was first rinsed by successive flushes with water and BGE for 2 and 3 min, respectively. Samples were introduced hydrodynamically by successively applying the pressure to the sample vial (30 mbar for 3 s, approximately, 4 nL), BGE vial (30 mbar for 1 s) and neutral marker vial (30 mbar for 3 s). The temperature in the capillary cartridge was set at 25°C. The voltage applied was 20 kV (positive polarity). The acquisition rate was 10 points/s. Analytes were detected by UV absorbance at 200 and 214 nm, according to cases. Capillaries were rinsed with water and dried by air when not in use.

For the determination of inclusion constant by ACE, samples were electrophoresed in serial BGEs containing increasing concentrations of CDs. Injections were repeated twice to check the precision of the data. Numerical data were processed using OriginPro 7.0 software (OriginLab Corporation, Northampton, USA) and Excel 2003 software (Microsoft Corporation, Redmond, USA).

For viscosity measurements of CD-containing BGEs used to calculate viscosity correction factor ν , a short plug (*ca.* 4 nL) of a flow marker, formamide, 0.03% v/v (3×10^{-5} mol/L) in the BGE, was first injected under a pressure of 30 mbar for 3 s in the BGE-filled capillary. The marker zone was next displaced by pushing the BGE under 50 mbar until the marker was detected. The measurement of the detection time of the marker, t_d , was used to calculate the viscosity according to Hagen-Poiseuille law

$$\eta = \frac{d_c^2 \Delta P t_d}{32lL} \quad (7)$$

where d_c stands for the inner diameter of the capillary, ΔP for the pressure applied, L and l for the total capillary length and length of detection window, respectively. The calibration of both the pressure delivery system and inner diameter of the capillary ($d_c^2 \cdot \Delta P$ term) was realized with solutions of ethyleneglycol ($\eta = 16.1 \times 10^{-3}$ Pa · s at 25°C) and diethyleneglycol ($\eta = 29.0 \times 10^{-3}$ Pa · s at 25°C).

4 Discussion

4.1 General experimental setup

The purpose of this work was to develop an ACE method for the determination of the inclusion parameters between imidazolium cations (Fig. 1) and different CDs and to provide data of relevance for imidazolium-based ILs. Mobility measurements were performed in a bare fused-silica capillary filled with a pH 5.0 acetate buffer of 30 mM ionic strength, keeping Joule heating within the dissipating capacity of the thermoregulation device. The experiments were carried out under positive polarity (20 kV), *i.e.*, in coelectroosmotic migration mode. A neutral marker (formamide) was injected in order to determine the effective mobility of the IL cations. A sequential injection protocol of the IL cation and the neutral marker was devised so that the neutral marker, which was injected second, would never be in contact with the IL cation, thus preventing any risk of deleterious interaction between them.

The viscosity measurements of each CD-containing BGEs were realized to calculate viscosity correction fac-

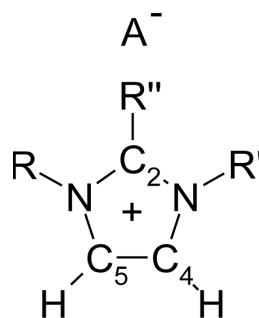
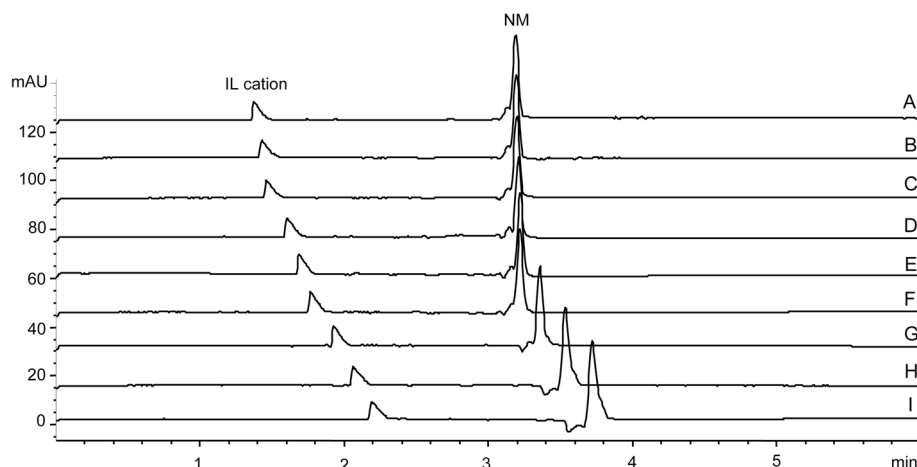


Figure 1. Ionic liquids studied in this work. 1-Ethyl-3-methylimidazolium bis(trifluoromethanesulfonyl)imide (R = Et, R' = Me, R'' = H, A = NTf₂), 1-butyl-3-methylimidazolium bis(trifluoromethanesulfonyl)imide (R = Bu, R' = Me, R'' = H, A = NTf₂), 1-butyl-3-methylimidazolium tetrafluoroborate (R = Bu, R' = Me, R'' = H, A = BF₄), 1-butyl-2,3-dimethylimidazolium tetrafluoroborate (R = Bu, R' = Me, R'' = Me, A = BF₄), 1-octyl-3-methylimidazolium bromide (R = C₈, R' = Me, R'' = H, A = Br), 1-decyl-3-methylimidazolium tetrafluoroborate (R = C₁₀, R' = Me, R'' = H, A = BF₄), 1-dodecyl-3-methylimidazolium tetrafluoroborate (R = C₁₂, R' = Me, R'' = H, A = BF₄).

Table 2. Modeling equation of the viscosity correction factor as a function of concentration for each CD used in this work at 25 °C

CDs	Viscosity correction factor	R ²
α -CD	$v = -453.2842 \times [\text{CD}]^3 + 50.48286 \times [\text{CD}]^2 + 0.62195 \times [\text{CD}] + 0.85923$	0.999
β -CD	$v = 2.16459 \times [\text{CD}] + 0.87687$	0.986
γ -CD	$v = -170.97535 \times [\text{CD}]^3 + 34.66408 \times [\text{CD}]^2 + 1.55085 \times [\text{CD}] + 0.88031$	0.999
HP- α -CD	$v = -950.16044 \times [\text{CD}]^3 + 86.77135 \times [\text{CD}]^2 + 1.25357 \times [\text{CD}] + 0.8792$	0.999
HP- β -CD	$v = 561.65047 \times [\text{CD}]^3 - 27.56666 \times [\text{CD}]^2 + 4.42357 \times [\text{CD}] + 0.87746$	0.999
HP- γ -CD	$v = 728.9039 \times [\text{CD}]^3 - 47.25401 \times [\text{CD}]^2 + 5.76565 \times [\text{CD}] + 0.87887$	0.999
DM- β -CD	$v = 1243.28674 \times [\text{CD}]^3 - 62.50023 \times [\text{CD}]^2 + 4.45666[\text{CD}] + 0.87708$	0.999
TM- β -CD	$v = -797.12969 \times [\text{CD}]^3 + 101.1041 \times [\text{CD}]^2 + 1.1649 \times [\text{CD}] + 0.87832$	0.999

**Figure 2.** Electropherograms showing the mobility shift of 1-octyl-3-methylimidazolium cation (C_8 MIM) as a function of α -CD concentration in the running buffer. A: Zero (neat background buffer); B: 1 mM; C: 2 mM; D: 3 mM; E: 5 mM; F: 10 mM; G: 20 mM; H: 30 mM; I: 50 mM. Experimental conditions: bare fused-silica capillary, 50 μm id \times 35 cm (detection cell, 26.5 cm). Running electrolyte: 30 mM sodium acetate buffer, pH 5.0 (ionic strength, 30 mM) containing α -CD at various concentrations (A–G). Applied voltage: 20 kV (current intensity: 50 μA). Temperature: 25 °C. Injection protocol: see Section 3.2. Sample: 2 mM C_8 MIM Br in the sodium acetate buffer, pH 5.0. NM: neutral marker.

tor v . The viscosity correction factor for the buffer system used in this work was related specifically to the concentration of each CD through a third-order polynomial, except for the β -CD, for which it can be calculated from a linear regression (Table 2).

According to the complexation stoichiometry, the inclusion constants were determined in this work both by direct nonlinear fitting of the binding isotherms and linear fittings of the linearized forms (case of a 1:1 stoichiometry), which permitted the evaluation of the quality of the experimental measurements, or by nonlinear fitting only (case of a 1:2 stoichiometry).

4.2 Imidazolium-based IL cation complexation by CDs

In order to investigate the inclusion complexation between imidazolium-based IL cations and CDs, seven methylimidazolium-based ILs differing in their alkyl chain length at the N1 position (C_2 – C_{12}), in the presence or the absence of a methyl group at the C2 position (Fig. 1) and in their anion nature (Br^- , BF_4^- , NTE_2^-) were

studied in the presence of eight different neutral CDs (α , β , γ , HP- α -, HP- β -, HP- γ -, DM- β -, and TM- β -CD). For each IL and according to the CD nature, the CD concentration added in the running buffer was varied over the range 0.1–50 mM. For the sake of example, Fig. 2 shows the electropherograms of C_8 MIM cation obtained with a bare silica capillary for various β -CD concentrations added to the running buffer. Upon increasing β -CD concentration, an increase in the migration time of the IL cation was observed, suggesting a decrease in the charge to mass ratio of the analyte. A similar electrophoretic behavior was observed for the other IL cation/CD systems, indicating the formation of a complex between these species. The peak tailing observed in Fig. 2 for C_8 MIM cation could be due to electromigration dispersion or also possibly to wall adsorption of IL cation, as reported [18] (*i.e.*, under conditions where wall adsorption is very unlikely due to the positive surface charge borne by this capillary). An identical series of experiments performed in a Polybrene modified capillary led, however, to the same K values as those obtained with bare silica capillary (results not shown), which indicated that wall adsorption, if pre-

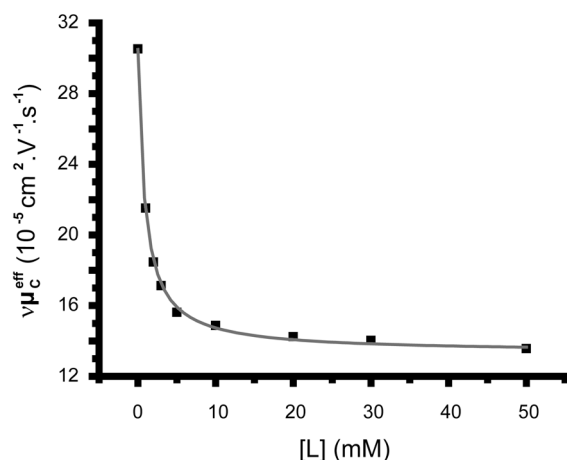


Figure 3. Variation of the effective mobility μ_c^{eff} (corrected for viscosity variations) of 1-octyl-3-methylimidazolium cation ($C_8\text{MIM}$) as a function of the $\alpha\text{-CD}$ concentration in the running electrolyte (binding isotherm plot). The solid line represents the nonlinear least-squares fitting of the data to Eq. (4). Experimental conditions, see Fig. 2.

sent, did not influence K determination with unmodified silica capillary. $C_8\text{MIM}$ cation peaks were then fitted with the Haarhoff Van der Linde function, allowing a better estimation of the migration time [44, 45]. As no significant difference was observed for the determination of the inclusion constant by using this treatment or by directly estimating the migration time from peak apex, this latter, simple method was employed subsequently.

The effective electrophoretic mobilities of the IL cations, μ_c^{eff} , were systematically calculated as a function of CD concentration. Direct nonlinear fitting (Fig. 3) to the binding isotherms (Eqs. 4 and 6) and linear fitting to the four linearized forms derived from Eq. (4) were then performed with these sets of mobility data for the determination of the complexation parameters.

Figure 4 shows the linear treatments performed with the experimental data pertaining to the $C_8\text{MIM}$ cation – $\alpha\text{-CD}$ system. The high degree of linear correlation obtained by the four linearization methods testifies to both the pertinency of the 1:1 complexation model and the precision of the experimental measurements. Simi-

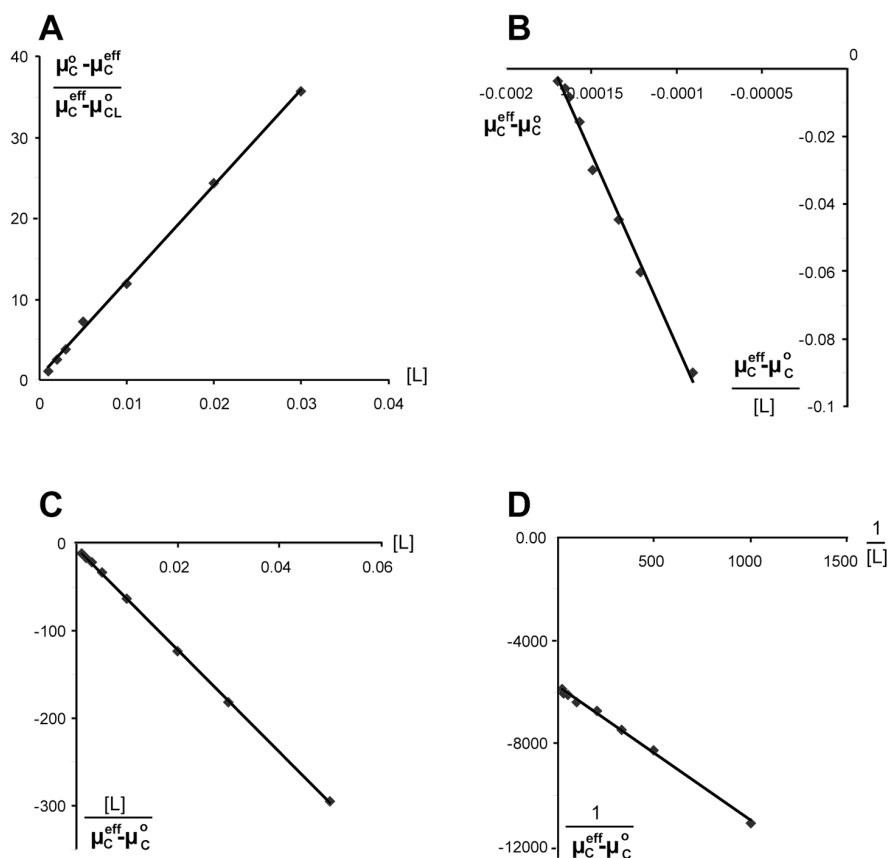


Figure 4. Linearized representations of the 1:1 binding isotherm for 1-octyl-3-methylimidazolium cation ($C_8\text{MIM}$), in the presence of variable concentrations of $\alpha\text{-CD}$: directly linearized isotherm (A), x -reciprocal (B), y -reciprocal (C), and double reciprocal (D) forms (see Table 1 for equations). Experimental conditions, see Fig. 2. Concentrations of ligand L ($\beta\text{-CD}$) in M and effective mobilities in $10^{-5} \text{ cm}^2 \text{ V}^{-1} \text{ s}^{-1}$.

Equations of the least-squares regression straight lines: A: $y = 1184.9x + 0.3542$, $R^2 = 0.999$, B: $y = -1133.2x - 0.1948$, $R^2 = 0.994$, C: $y = -5820.1x - 5.3491$, $R^2 = 0.999$, D: $y = -5.2051x - 5801.2$, $R^2 = 0.997$.

Table 3. Step by step inclusion constants K_1 and K_2 of imidazolium-based IL cations with neutral CDs, as determined by the ACE mobility shift method, using four linearization plotting methods, and a nonlinear fitting method to Eqs. (4) and (6). Experimental conditions as in Fig. 2. Linearized equations of the 1:1 binding isotherm as mentioned in Table 1

	K_1 (M^{-1}) Eq. (4)	K_1 (M^{-1}) Isotherm method	K_1 (M^{-1}) x -Reciprocal method	K_1 (M^{-1}) y -Reciprocal method	K_1 (M^{-1}) Double reciprocal method	Average value for K_1 (M^{-1}) $\pm \sigma^a$	$K_1; K_2$ (M^{-1}) Eq. (6) $\pm \sigma^a$
α -CD							
EMIM NTf ₂	0	0	0	0	0	0	
BMIM BF ₄	29	31	27	26	28	28 \pm 4	
BMIM NTf ₂	32	32	26	26	26	28 \pm 5	
BMMIM BF ₄	33	30	27	28	25	28 \pm 4	
C ₈ MIM Br	1130	1185	1130	1160	1115	1148 \pm 70	
C ₁₀ MIM BF ₄							2900 \pm 320; 3 \pm 2
C ₁₂ MIM BF ₄							6870 \pm 280; 51 \pm 12
β -CD							
EMIM NTf ₂	0	0	0	0	0	0	
BMIM BF ₄	0	0	0	0	0	0	
BMIM NTf ₂	0	0	0	0	0	0	
BMMIM BF ₄	0	0	0	0	0	0	
C ₈ MIM Br	643	680	657	712	639	672 \pm 50	
C ₁₀ MIM BF ₄	2914	3211	3372	2223	3346	3038 \pm 290	
C ₁₂ MIM BF ₄	9910	10891	10026	13029	10028	10 994 \pm 600	
γ -CD							
EMIM NTf ₂	0	0	0	0	0	0	
BMIM BF ₄	0	0	0	0	0	0	
BMIM NTf ₂	0	0	0	0	0	0	
BMMIM BF ₄	0	0	0	0	0	0	
C ₈ MIM Br	0	0	0	0	0	0	
C ₁₀ MIM BF ₄	107	105	107	104	106	106 \pm 3	
C ₁₂ MIM BF ₄	250	230	255	230	260	244 \pm 20	
HP- α -CD							
EMIM NTf ₂	0	0	0	0	0	0	
BMIM BF ₄	13	15	11	11	10	12 \pm 2	
BMIM NTf ₂	12	15	10	10	9	11 \pm 2	
BMMIM BF ₄	15	20	12	13	10	14 \pm 2	
C ₈ MIM Br	527	630	644	660	633	642 \pm 50	
C ₁₀ MIM BF ₄	2062	2802	2334	2904	2310	2588 \pm 200	
C ₁₂ MIM BF ₄	4467	4846	5552	4657	5563	5155 \pm 350	
HP- β -CD							
EMIM NTf ₂	0	0	0	0	0	0	
BMIM BF ₄	0	0	0	0	0	0	
BMIM NTf ₂	0	0	0	0	0	0	
BMMIM BF ₄	0	0	0	0	0	0	
C ₈ MIM Br	225	256	260	269	255	260 \pm 20	
C ₁₀ MIM BF ₄	1190	1322	1389	1430	1367	1377 \pm 90	
C ₁₂ MIM BF ₄	4321	5228	5558	4350	5647	5196 \pm 550	
HP- γ -CD							
EMIM NTf ₂	0	0	0	0	0	0	
BMIM BF ₄	0	0	0	0	0	0	
BMIM NTf ₂	0	0	0	0	0	0	
BMMIM BF ₄	0	0	0	0	0	0	
C ₈ MIM Br	14	20	14	14	14	16 \pm 3	
C ₁₀ MIM BF ₄	60	70	65	75	63	68 \pm 6	
C ₁₂ MIM BF ₄	230	225	235	241	240	235 \pm 20	
DM- β -CD							
EMIM NTf ₂	0	0	0	0	0	0	
BMIM BF ₄	0	0	0	0	0	0	

Table 3. Continued ...

	K_1 (M^{-1}) Eq. (4)	K_1 (M^{-1}) Isotherm method	K_1 (M^{-1}) x -Reciprocal method	K_1 (M^{-1}) y -Reciprocal method	K_1 (M^{-1}) Double reciprocal method	Average value for K_1 (M^{-1}) $\pm \sigma^a$	$K_1; K_2$ (M^{-1}) Eq. (6) $\pm \sigma^a$
BMIM NTf ₂	0	0	0	0	0	0	
BMMIM BF ₄	0	0	0	0	0	0	
C ₈ MIM Br	717	720	710	660	690	695 ± 70	
C ₁₀ MIM BF ₄							2620 ± 290; 17 ± 6
C ₁₂ MIM BF ₄							8685 ± 1050; 11 ± 3
TM-β-CD							
EMIM NTf ₂	0	0	0	0	0	0	
BMIM BF ₄	0	0	0	0	0	0	
BMIM NTf ₂	0	0	0	0	0	0	
BMMIM BF ₄	0	0	0	0	0	0	
C ₈ MIM Br	70	75	67	67	64	68 ± 4	
C ₁₀ MIM BF ₄	280	245	260	280	250	259 ± 20	
C ₁₂ MIM BF ₄	892	789	872	794	855	828 ± 80	

^{a)} σ : SDs as calculated from x -reciprocal treatment ($n = 10$ for a given IL)

lar conclusions can be drawn for the majority of studied imidazolium cations and CDs, displaying correlation coefficients in excess of 0.990 for all the linear regression performed, but in four cases (see below) the fittings to these linearized equations failed to produce linear plots. Interestingly, better correlation coefficients were obtained in these cases by nonlinear fitting to Eq. (6), corresponding to a 1:2 complexation stoichiometry. Table 3 summarizes the complexation constants obtained by each plotting method for all the studied IL cation-CD systems. It should be emphasized that for 1:1 complexations, close values of formation constants were generally obtained by the various linear and nonlinear plotting methods, although in some cases one of them yielded a result which was somewhat different from the other ones. As the method yielding this, apparently more scattered result was not the same for the different IL cations, we deemed it better to express the results as the average of the values provided by the five methods. Thus, the use of the five plotting methods seemed preferable for a more reliable determination of the complexation constant.

The results given in Table 3 show, for each CD, a pronounced increase in the K_1 value in the order: EMIM < BMIM ~ BMMIM < C₈MIM < C₁₀MIM < C₁₂MIM. This order emphasized the prominent role of the alkyl chain length of the IL cation in the inclusion mechanism. The nil K_1 values obtained for EMIM cation with all the CDs demonstrate that there is no inclusion of the imidazolium ring into the CD cavity, whatever its size (α -, β -, γ -CDs). In addition, the very close results obtained for BMIM BF₄ and BMMIM BF₄ do not allow to conclude to a significant influence of the presence of a methyl group at the C2 position. Eventually, the nature and length of the side alkyl chain of the IL cation is by far the major parameter

controlling inclusion. These results are in agreement with those by Rekharsky *et al.* [46], which did not emphasize any complexation phenomenon between imidazolium cation and α - or β -CD.

As exemplified by studies of BMIM NTf₂ and BMIM BF₄ IL samples in the presence of α -CD and HP- β -CD, the nature of the anion initially associated to the imidazolium cation in the IL sample did not show any significant influence on K_1 values obtained. This result can be anticipated in so far as a short plug of dilute IL sample was introduced for the assay and the acetate buffer anion common to all the experiments was present in large excess.

The differences in main properties between the three natural CDs and the CD derivatives used in this study, made it difficult to compare K_1 values obtained for a given IL cation and different CDs, but these results can be compared according to the CD cavity size for a given type of substituting moiety. For the sake of example, Fig. 5 shows a histogram representation of the K_1 values for C₈MIM cation obtained with each CD. For the 1:1 complexation stoichiometry model, a pronounced decrease in the K_1 value in the order: α -CD > β -CD > γ -CD, HP- α -CD > HP- β -CD > HP- γ -CD, and DM- β -CD > TM- β -CD, respectively, was observed. This order for the natural CD and HP-CD groups emphasized the prominent role of CD cavity size in the inclusion mechanism. As support by the physical properties recalled in Table 4, which can be considered as approximately valid for HP-CDs [47], K_1 values markedly decrease when the cavity diameter increases. Figure 5 also shows a higher K_1 value for C₈MIM with DM- β -CD as compared to TM- β -CD. This result is probably due to a more important steric hindrance of TM- β -CD cavity. Moreover, methylated β -CDs are known to be more hydrophobic and to have a deeper cavity than γ -CD [48,

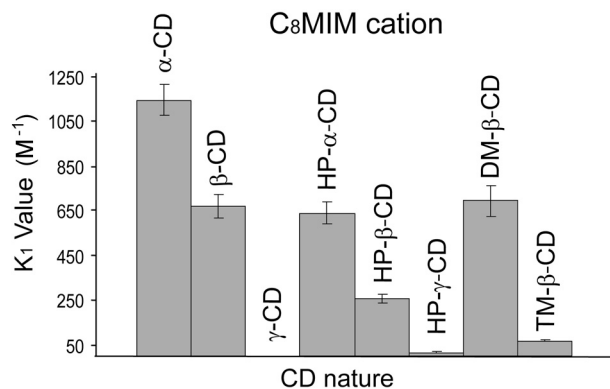


Figure 5. Histogram representing the K_1 value for 1-octyl-3-methylimidazolium cation (C_8 MIM) as a function of the CD nature, bars represent SD. Experimental conditions, see Fig. 2.

Table 4. Main physical properties of native CDs [44]

	α	β	γ
Number of glucose units	6	7	8
Molecular mass	972.8	1135.0	1297.1
Inner diameter of the cavity (Å)	4.7–5.3	6.0–6.5	7.5–8.3
Diameter of outer periphery (Å)	14.6 ± 0.4	15.4 ± 0.4	17.5 ± 0.4
Height of torus (Å)	7.9 ± 0.1	7.9 ± 0.1	7.9 ± 0.1
Approximate volume of cavity (Å ³)	174	262	427

49]. Similar conclusions can be drawn for the majority of studied imidazolium cations and CDs for the 1:1 complexation stoichiometry model.

For the longer alkyl chains at the N1 position experienced (C_{10} and C_{12}) and in cases concerning complexation by α -CD and DM- β -CD, much better correlation of the experimental data was obtained with the 1:2 complexation stoichiometry model rather than with the 1:1 model. Such situation, although rare, where two CDs bind a single guest molecule, has already been reported for some molecularly favorable cases [50–52]. Especially, Funasaki *et al.* recently evidenced 1:2 complexes between long chain surfactant and CDs by NMR studies and proposed a head-to-head position of the CD dimer in the 1:2 complex [53–55]. Although the exact interaction mode involved in our ternary systems cannot be ascertained simply from these experiments, it can be inferred that two CD molecules may be threaded likewise along the alkyl side chain, as outlined in Fig. 6.

5 Conclusion

An ACE method has been developed for the determination of the inclusion parameters between seven alkyl(methyl)methylimidazolium cations and eight neutral

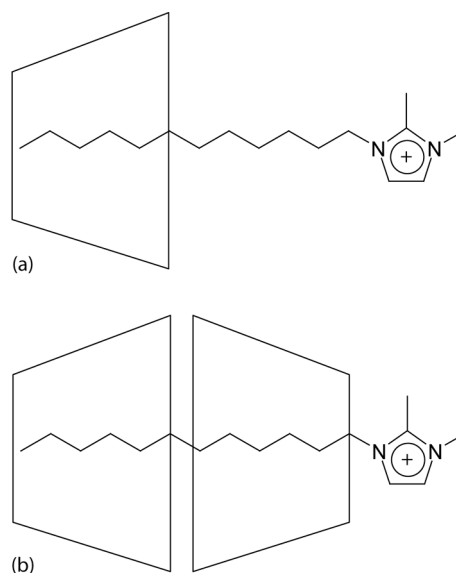


Figure 6. Schematic representation of (a) the 1:1 and (b) 1:2 complexes between alkyl(methyl)methylimidazolium cation and CDs, as inferred from ref. [55].

CDs. The majority of systems followed a 1:1 complexation stoichiometry model but in four cases a 1:2 stoichiometry was highlighted. By studying these 56 possible IL/CD systems, it was established that the main factor influencing the strength of the inclusion complexation was the length of alkyl side chain on the imidazolium ring. The presence of a methyl group at the C2 position and the nature of anion associated to the imidazolium cation in the IL did not show significant influence on the complexation constant obtained. Also, the size of the CD cavity noticeably impacts the stability of the 1:1 complexes, with stronger complexes being given by α -CD. Finally, it was shown that two CD molecules can likely be threaded along C_{10} and C_{12} alkyl side chains. The availability of these data should be of support in various application areas, including the screening and tailoring of new interactions in solution for CE.

6 References

- [1] Wasserscheidt, P., Weldon, T., *Ionic Liquids in Synthesis*, Wiley-VCH, New-York 2003.
- [2] Dupont, J., de Souza, R. F., Suarez, P. A. Z., *Chem. Rev.* 2002, 102, 3667–3692.
- [3] Wasserscheidt, P., Keim, W., *Angew. Chem. Int. Ed.* 2000, 39, 3772–3789.
- [4] Earle, M. J., Seddon, K. R., *Pure Appl. Chem.* 2000, 72, 1391–1398.
- [5] Cull, S. G., Holbrey, J. D., Vargas-Mora, V., Seddon, K. R., Lye, G. J., *Biotechnol. Bioeng.* 2000, 69, 227–233.
- [6] Huddleston, J. G., Willauer, H. D., Swatloski, R. P., Visser, A. E., Rogers, R. D., *Chem. Commun.* 1998, 1765–1766.
- [7] Fadeev, A. G., Meagher, M. M., *Chem. Commun.* 2001, 295–296.

- [8] Berthod, A., Ruiz-Angel, M. J., Hugué, S., *Anal. Chem.* 2005, 77, 4071–4080.
- [9] Visser, A. E., Swatloski, R. P., Rogers, R. D., *Green Chem.* 2000, 2, 1–4.
- [10] Pachole, F., Butler, H. T., Poole, C. F., *Anal. Chem.* 1982, 54, 1938–1941.
- [11] Andersen, J. L., Ding, J., Welton, T., Armstrong, D. W., *J. Am. Chem. Soc.* 2002, 124, 14247–14254.
- [12] Berthod, A., He, L., Armstrong, D. W., *Chromatographia* 2001, 53, 63–68.
- [13] Heintz, A., Kulikov, D. W., Verevkin, S. P., *J. Chem. Eng. Data* 2002, 47, 894–899.
- [14] He, L., Zhang, W., Zhao, L., Liu, X., Jiang, S., *J. Chromatogr. A* 2003, 1007, 39–45.
- [15] Kalisz, R., Marszall, M. P., Markuszewski, M. J., Baczek, T., Permak, J., *J. Chromatogr. A* 2004, 1030, 263–271.
- [16] Xiao, X., Zhao, L., Liu, X., Jiang, S., *Anal. Chim. Acta* 2004, 519, 207–211.
- [17] Yanes, E. G., Gratz, S. R., Stalcup, A. M., *Analyst* 2000, 125, 1919–1923.
- [18] Yanes, E. G., Gratz, S. R., Baldwin, M. J., Robinson, S. E., Stalcup, A. M., *Anal. Chem.* 2001, 73, 3838–3844.
- [19] Vaher, M., Koel, M., Kaljurand, M., *Chromatographia* 2001, 53, 302–306.
- [20] Vaher, M., Koel, M., Kaljurand, M., *Electrophoresis* 2002, 23, 426–430.
- [21] Vaher, M., Koel, M., Kaljurand, M., *J. Chromatogr. A* 2002, 979, 27–32.
- [22] Kuldvee, R., Vaher, M., Koel, M., Kaljurand, M., *Electrophoresis* 2003, 24, 1627–1634.
- [23] Vaher, M., Koel, M., *J. Chromatogr. A* 2003, 990, 225–230.
- [24] Qi, S., Cui, S., Chen, X., Hu, Z., *J. Chromatogr. A* 2004, 1059, 191–198.
- [25] Qi, S., Li, Y., Deng, Y., Cheng, Y., *et al.*, *J. Chromatogr. A* 2006, 1109, 300–306.
- [26] Mwangi, S. M., Numan, A., Gill, N. L., Agbaria, R. A., Warner, I. M., *Anal. Chem.* 2003, 75, 6089–6096.
- [27] Tran, C. D., De, Paoli Lacerda, S. H., *Anal. Chem.* 2002, 74, 5337–5341.
- [28] Armstrong, D. W., He, L., Liu, Y.-S., *Anal. Chem.* 1999, 71, 3873–3876.
- [29] Tanaka, Y., Terabe, S., *J. Chromatogr. B* 2002, 768, 81–92.
- [30] Rippel, G., Corstjens, H., Billiet, H. A. H., Frank, J., *Electrophoresis* 1997, 18, 2175–2184.
- [31] Schou, C., Heegaard, N. H. H., *Electrophoresis* 2006, 27, 44–59.
- [32] Rundlett, K. L., Armstrong, D. W., *Electrophoresis* 1997, 18, 2194–2202.
- [33] Rundlett, K. L., Armstrong, D. W., *Electrophoresis* 2001, 22, 1419–1427.
- [34] Bowser, M. T., Chen, D. D. Y., *Anal. Chem.* 1998, 70, 3261–3270.
- [35] Connors, K. A., *Binding Constants. The Measurements of Molecular Complex Stability*, John Wiley & Sons, New York 1987.
- [36] Rundlett, K. L., Armstrong, D. W., *J. Chromatogr. A* 1996, 721, 173–186.
- [37] Vespalec, R., Bocek, P., *J. Chromatogr. A* 2000, 875, 431–445.
- [38] Bowser, M. T., Sternberg, E. D., Chen, D. D. Y., *Electrophoresis* 1997, 18, 82–91.
- [39] Bowser, M. T., Chen, D. D. Y., *J. Phys. Chem. A* 1999, 103, 197–202.
- [40] Cammarata, I., Kazarian, S. G., Salter, P. A., Welton, T., *Phys. Chem. Chem. Phys.* 2001, 3, 5192–5200.
- [41] Yao, Y. J., Li, S. F. Y., *J. Chromatogr. A* 1994, 680, 431–435.
- [42] Cordova, E., Gao, J., Whitesides, G. M., *Anal. Chem.* 1997, 69, 1370–1379.
- [43] Macia, A., Borrull, F., Calull, M., Aguilar, C., *Electrophoresis* 2004, 25, 3441–3449.
- [44] Erny, G., Bergström, E., Goodall, D., Grieb, S., *Anal. Chem.* 2001, 73, 4862–4872.
- [45] Le Saux, T., Varenne, A., Gareil, P., *Electrophoresis* 2005, 26, 3094–3104.
- [46] Rekharsky, M. V., Nemykina, E. V., Eliseev, A. V., Yatsimirski, A. K., *Thermochim. Acta* 1992, 202, 25–33.
- [47] Szejtli, J., *Pure Appl. Chem.* 2004, 76, 1825–1847.
- [48] Nishiho, J., Shiota, S., Mazima, K., Inoue, Y., *et al.*, *Chem. Pharm. Bull.* 2000, 48, 48–55.
- [49] Szejtli, J., *Cyclodextrin Technology*, Kluwer Academic Publisher, Dordrecht 1988.
- [50] Armstrong, D. W., Nome, F., Spino, L. A., Golden, T. D., *J. Am. Chem. Soc.* 1986, 108, 1418–1421.
- [51] Connors, K. A., Pendergast, D. D., *J. Am. Chem. Soc.* 1984, 106, 7607–7614.
- [52] Wan Yunus, W. M. Z., Taylor, J., Bloor, D. M., Hall, D. G., Wyn-Jones, E., *J. Phys. Chem.* 1992, 96, 8979–8982.
- [53] Funasaki, N., Neya, S., *Langmuir* 2000, 16, 383–388.
- [54] Funasaki, N., Ishikawa, S., Neya, S., *J. Phys. Chem. B* 2004, 108, 9593–9598.
- [55] Funasaki, N., Ishikawa, S., Hirota, S., *Anal. Chim. Acta* 2006, 555, 278–285.